Int J Adv Manuf Technol (2009) 43:1144–1156
DOI 10.1007/s00170-008-1793-x

ORIGINAL ARTICLE

Development of a MIAB welding module and experimental analysis of rotational behavior of arc—simulation of electromagnetic force distribution during MIAB welding of steel pipes using finite element analysis

S. Arungalai Vendan · S. Manoharan · G. Buvanashekaran · C. Nagamani

Received: 20 May 2008 / Accepted: 6 October 2008 / Published online: 4 November 2008

Abstract Magnetically impelled arc butt (MIAB) welding is a unique forge welding process in which an arc is drawn in the gap between the two tubes to be welded in order to raise them to a high temperature to allow forging to form a solid-state weld. In this case, the arc is rotated with a high speed around the weld line by an electromagnetic force resulting from the interaction of the magnetic field and the arc current. This paper presents the details of the results and the conclusions of the experimental trials conducted on the MIAB module designed and developed based on the principle. Further, nonlinear electromagnetic analysis has been performed to determine the magnetic field and electromagnetic force distribution in MIAB process using finite element package ANSYS. Typical results of this analysis pertaining to magnetic field are compared with the experimental data for steel tubes (outer diameter 47 mm and thickness of 2 mm). It is observed that the results from finite element analysis and the experimental trials are in excellent agreement. The proposed three-dimensional finite element method model for electromagnetic force distribution facilitates comprehensive understanding of the arc rotation process in MIAB welding.

S. A. Vendan (✉) · C. Nagamani
Department of Electrical and Electronics Engineering,
National Institute of Technology,
Tiruchirappalli, 620015, India
e-mail: arungalaisv@yahoo.co.in

S. Manoharan · G. Buvanashekaran
Welding Research Institute, BHEL,
Tiruchirappalli, 620015, India

Keywords MIAB welding · Electromagnetic force · Magnetic flux density · ANSYS · Finite element analysis

1 Introduction

The magnetically impelled arc butt (MIAB) welding process was initially investigated by the E.O. Paton Electric Welding Institute during the 1950s and 1960s. It was later developed for commercial applications by Kuka Welding systems, who named it the magnetarc process. Today, MIAB welding is used for a variety of applications throughout Europe and the Ukraine, and Paton continues its MIAB research and development efforts. MIAB process is being applied in different industries for manufacture of hollow parts, such as pneumatic springs, cardan shaft, shock absorbers, vacuum amplifiers of brakes, reactive rod, and other parts of the auto industry.

MIAB welding is a unique process which utilizes relatively simple equipment but relies on very complex interactions between an arc and both an applied and induced magnetic field. This interaction is made even more complex by the changes that occur during the heating of the parts being welded. The result is a very swift welding process that offers cost savings for a range of joint configurations. Welding of tubular components employing MIAB welding process involves the tubular components to be clamped in line with a gap of about 2 to 3 mm between them. Then, a magnetic field is established into the gap by an external magnetic system. A conventional arc welding power source produces an arc between the two faying surfaces of the tubes, and the arc begins to rotate around the tubes because of the applied magnetic field. The arc accelerates swiftly up to a linear speed

of 200 m/s, when it attains a steady speed. To an observer, a continuous glowing arc appears to completely fill the space between the tubes. The rotating arc generates a continuous heating effect instantly and the ends of the tubes become red hot. At that moment, the tubular components are forged together to make the weld and the arc is extinguished. The properly clamped tubular components are not rotated or displaced so that alignment is maintained. Very little dispersion is produced, making it an immaculate process. The process can be used to weld non-circular components that may not be suitable for friction welding. The total time for the completion of the weld depends on the diameter and the wall thickness.

MIAB has been reported in literature as early as 1974. From the available literature, the work carried out previously by the researchers on MIAB welding is discussed below.

Ganowski [1] presented a survey of the state of magnetic arc welding process and its mechanical development. Georgescu et al. [2] presented the principle of ROTARC welding and discussed details of several original equipment developed by them. In addition, the experimental results with a classical longitudinal magnetizing system and the conclusions of the experiments were presented. Glickstein [3] developed a one-dimensional model of the welding arc that considers heat generation by the joule effect and heat losses by radiation and conduction in order to study the effects of various gases and gas mixtures for welding applications. Kim and Choi [4] developed a two-dimensional finite element model for the analysis of magnetic flux density distributions produced by electromagnets at the MIAB weld joint. The primary objective was to establish a relationship between the strength of the radial magnetic field at the joint and the quality of the weld joint between two steel pipes. Vendan et al. [5] reported the simulation of magnetic flux distribution for magnetically impelled arc butt welding of steel pipes. This concept was based on the knowledge that a stronger magnetic field produces a higher force on the arc, resulting in faster arc speed and more uniform heating. Also, the same group [6] carried out modeling of magnetic flux distribution for magnetically impelled arc butt welding of steel tubes using finite element analysis. The relation between magnetic flux density and the parameters governing them in a MIAB welding process of steel tubes were illustrated with a three-dimensional finite element method (FEM) model. Georgescu and Oirdachescu [7] presented a compact design and development of a portable equipment for rotary arc operated pneumatically. The equipment was designed for welding a maximum of 30-mm diameter pipes. Schlebeck [8] reported welding with a magnetically moved arc (MBL welding). The technical state of development of MBL-P welding (welding with magnetically moved arc with pressure force), machines and power sources for MBL-P welding quality of the MBL-P weld joints were also described. The work of Yatsenko et al. [9] focused on developing new method of a MIAB welding of pipes with a higher wall thickness exceeding the sizes of active spots of arc columns. A mechanical property of welded joints of pipes of 16-mm wall thickness was discussed. Kachinskiy et al. [10] discussed the developments in the field of MIAB welding of different compositions of steel and for hollow shapes with wall thicknesses over 10 mm and also for solid parts used in pipeline construction, in automobile, and other industries. Johnson et al. [11] reported an evaluation of a commercially available MIAB machine used for welding 51-mm (2 in.) diameter, 3-mm (0.12 in.) wall mild steel tubing. The quality of MIAB welds were assessed by bend testing and by the height of the internal upset. Tagaki et al. [12] reported the development of rotating arc welding equipment suited for application to town gas pipelines. In this study, it has been proven that welds of high quality and reliability can be obtained with high efficiency and that the welding equipment can be used very effectively in pipeline laying. Mori and Yasuda [13] described the MIAB welding process developed for welding non-ferrous metals such as aluminum and copper, which are non-ferromagnetic.

Although several studies [1–13] had reported MIAB welding, very little has been mentioned about the design and development of a laboratory test module for MIAB welding process. An attempt is made here to develop a laboratory module for MIAB welding and to propose a FE-based three-dimensional model for determining the magnetic flux density and electromagnetic force distribution, respectively, which are the key parameters in the MIAB welding process. Further, experimental data are utilized to verify the proposed FEM model. The excellent correlation between the results of numerical analysis (proposed FEM model) and the experimental results establish the validity of the proposed FEM model.

The paper is organized as follows. Section 2 discusses in detail the theory involved in MIAB welding process. Section 3 deals with the elaborate description of the various stages implicated in MIAB welding process. Section 4 provides the chemical composition of the test specimen used for the experimental purpose. Section 5 presents the particulars of the trials conducted along with the photographs of the designed MIAB laboratory module. Section 6 revolves around the aspects concerned with the development of three-dimensional finite element analysis (FEA) model for performing simulation of MIAB welding process to explore the magnetic flux and electromagnetic force distribution, respectively, in MIAB welding process. Section 7 provides particulars about some of the results obtained in experimental trail carried out on the designed MIAB laboratory module and few FEM simulation results. Further, the possible reasons leading to the observed result

are discussed in detail. Section 8 deals with the measuring method which is employed in investigating and validating the results obtained through FEM simulation. The interpretations made from experimental and simulation results are presented in Section 9.

2 Principle of MIAB welding process

MIAB welding is a fusion welding process for tubes and pipes in which heat is generated prior to forging by an electric arc moving along the peripheral edges of the weldments with the aid of an external magnetic field. The schematic diagram depicting the principle of MIAB welding process is shown in Fig. 1.

Two tubes to be welded are clamped with proper alignment. The magnetic systems incorporated in the MIAB welding module produce magnetic flux in the arc gap. The radial component of the magnetic flux density, B_r, and the axial component of the welding arc current, I_a, interact with each other, leading to the generation of an electromagnetic force. The mathematical expression of this electromagnetic force is given in Eq. 1.This force impels the arc along the peripheral edges of the tubes.

$$\vec{F}_{B_r} = K \times \vec{I}_a \times \vec{B}_r. \quad (1)$$

Coefficient K depends on the value of the arc gap between the two tubes to be welded.

The direction of the force is determined by applying Fleming's left hand rule, which states that the rotating direction of the arc is always perpendicular to the applied magnetic field and the arc current as shown in Fig. 2.

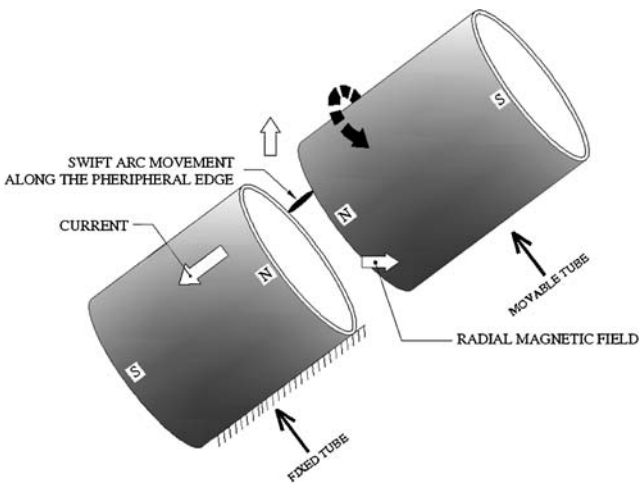

Fig. 1 Schematic representation of MIAB welding process

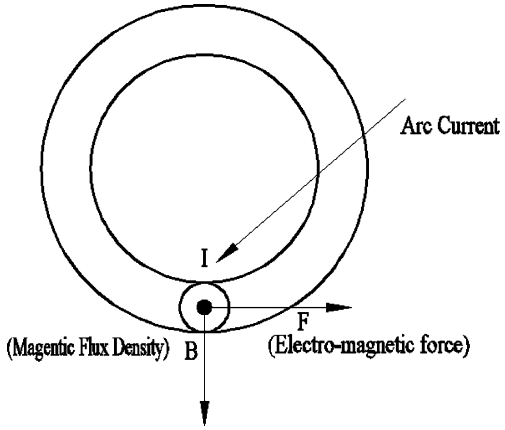

Fig. 2 Fleming's left hand rule [4]

3 Sequence of operations in MIAB welding

MIAB welding is a pressure welding technique using either electromagnets or permanent magnets to impel the arc along the faying surfaces to be welded. The sequence of the joining process can be divided into the following phases:

Phase 1: The clamped work pieces and the external magnetic coil system installed in the area of the joint and which does not come in contact with the workpieces is shown in Fig. 3.

Phase 2: The clamped workpieces are brought into contact before the magnetic coil and welding current is switched ON as shown in Fig. 4. The gap between the tubes is zero now.

Phase 3: The magnetic coil and welding current have been switched ON and the workpieces are retracted to produce a defined gap, thereby striking an arc as shown in Fig. 5. The gap between the tubes is nearly 2 mm.

Phase 4: The magnetic field of the coil causes the arc to rotate about the interface. The abutting faces are thus uniformly heated and melted. A single arc picking up acceleration and rotating faster is shown in Fig. 6.

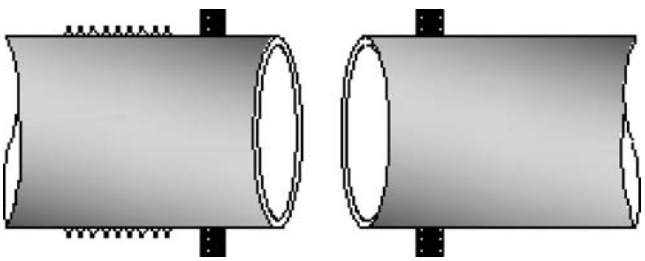

Fig. 3 Magnetically impelled arc butt welding—phase 1

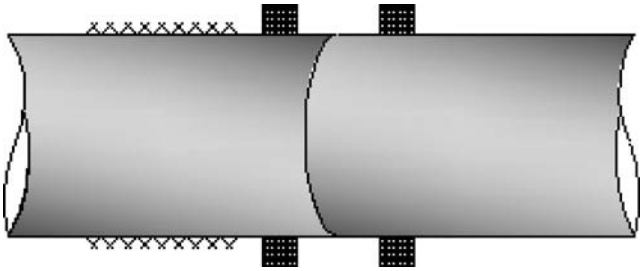

Fig. 4 Magnetically impelled arc butt welding—phase 2

Phase 5: The melted abutting faces are pressed together by a forging cylinder. The tubular materials are then joined forming a porosity-free weld as shown in Fig. 7. The magnetic coil and welding current are switched OFF.

4 Specimen for experimentation

For all the experimental trials, T11 grade tubes having chromium alloying are used. This grade is selected since the pressure vessel application requires high-temperature properties during their life cycle. The chemical composition of T11 is given in Table 1

5 Experimental study

In the MIAB setup developed in the laboratory, one of the tubes is fixed and the other tube is movable, as shown in Fig. 8a. The linearly movable tube is coupled to an electric motor. Using the movable jaw, the distance between the tubes is adjusted in the range of 10–15 mm. Magnetic coil arrangement is shown in Fig.8b, which comprises a laminated core on which a coil is wound. When power supply is given, the arc strikes between the tubes and rotates at a low speed of about 75 rpm.

Several trials are conducted with the welding current in the range of 400–500 A, with the welding voltage in the range 90–120 V. ESAB power source is used for this purpose. The coil (electromagnet) is supplied from a variable dc source of 75–200 V and 0.1–0.5 A. Trials show that arc rotation with this arrangement of the magnetic coils is continuous and uniform. This arrangement facilitates around 50% to 60% of the melting job. Further, an upset force of 30 to 100 N/mm^2 to join the tubes is found to be adequate.

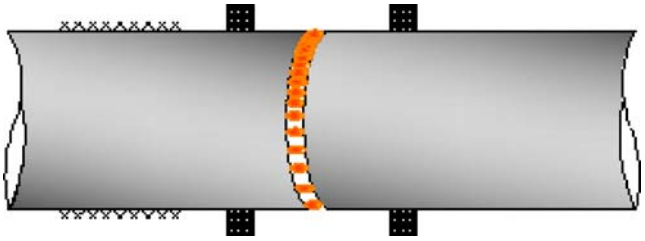

Fig. 6 Magnetically impelled arc butt welding—phase 4

Further, the entire magnetic coil setup was modified in order to achieve a better arc rotation. Instead of laminated core as used previously, solid core design is used because of magnetic saturation problem as shown in Fig. 9. A 56-mm diameter tube was cut into two halves and placed at the ends of the solid core. In this MIAB module, arc rotation is uniform and it is comparatively faster. With the laboratory MIAB setup, the arc rotation behavior mainly depended upon the parameters like gap size, coil position, and exciting current.

6 Finite element analysis

The finite element analysis package ANSYS provides a way to simulate the loading conditions in any selected system design and determine the design's response to those conditions. It is convenient to numerically model MIAB welding system using finite element analysis. The solution technique is selected depending on the type of problem.

The geometry, node locations, and the coordinate system for this element are shown in Fig. 10. The element is defined by eight nodes and has up to four degrees of freedom per node: z component of the magnetic vector

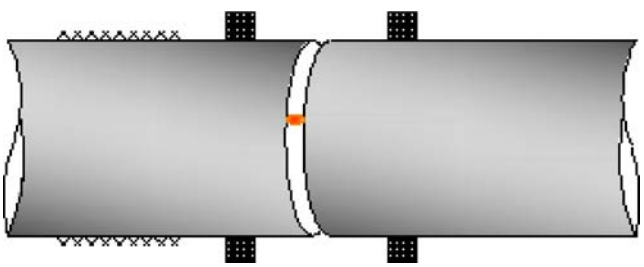

Fig. 5 Magnetically impelled arc butt welding—phase 3

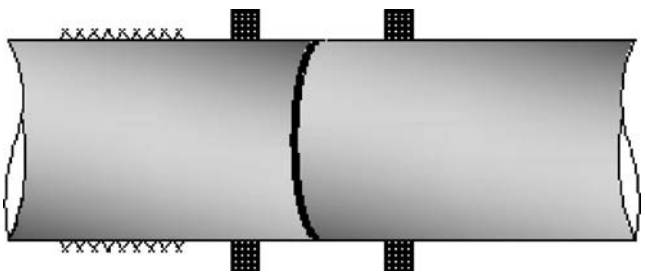

Fig. 7 Magnetically impelled arc butt welding—phase 5

Table 1 Chemical composition (T11) of tubes

C	Mn	P	S	Si	Mb	Cr
0.05–0.15	0.30–0.60	0.025	0.020	0.50–1.00	0.44–0.65	1.00–1.5

potential (AZ), time-integrated electric scalar potential (VOLT), electric current (CURR), and electromotive force (EMF). The element is based on the magnetic vector potential formulation and is applicable to the following low-frequency magnetic field analyses: magneto statics, eddy currents (AC time harmonic and transient analyses), voltage-forced magnetic fields (static, AC time harmonic and transient analyses), and electromagnetic-circuit-coupled fields (static, AC time harmonic and transient analyses). The element has nonlinear magnetic capability for modeling B–H curves or permanent magnet demagnetization curves. The element input data include eight nodes and the magnetic material properties (nonlinearity). Figure 11 shows the B–H curve of the test specimen. Newton–Raphson solution approach is adopted.

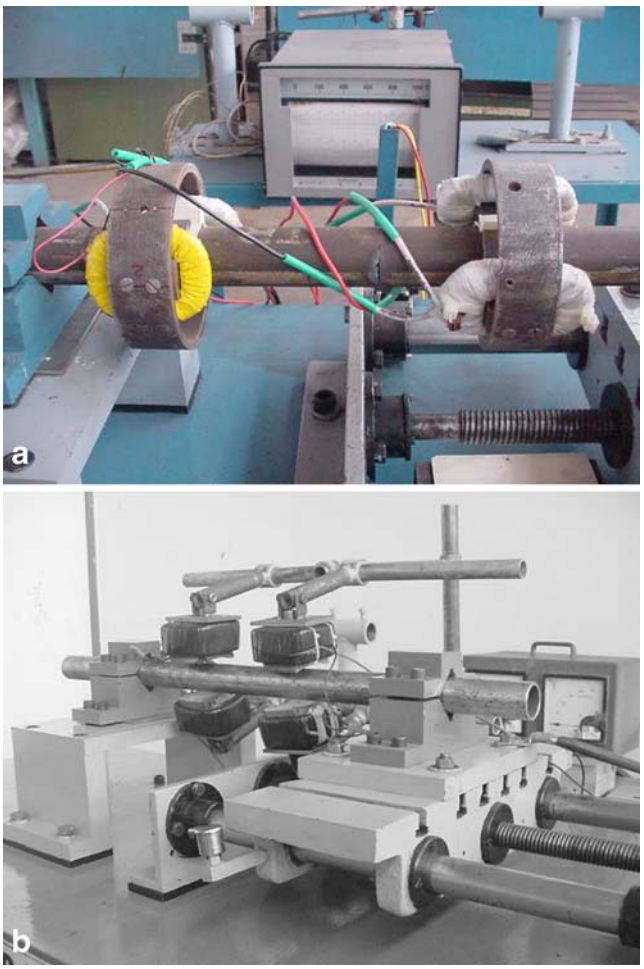

Fig. 8 MIAB welding module

Fig. 9 MIAB welding module (modified)

Finite element analysis is employed for examining the radial magnetic flux density distribution in the tube gap for different sets of the exciting current in the coils and the center to coil distance [5]. A three-dimensional finite element model is adopted for the analyses shown in Fig. 12 in which the mesh system in the vicinity of the exciting coils is represented.

This finite element model includes a total of 75,675 nodes and 24,998 elements for the calculation domain. The calculation domain was increased and selected through a series of calculations for this size, which showed a converging distribution of magnetic flux density. The boundary condition is that there is no magnetic flux on the outside of the calculation domain.

7 Results and discussion

The primary focus of this work was to investigate the magnetic flux density distribution and the electromagnetic force in the MIAB welding process followed by parametric evaluation through simulations and experimentation. The results both from the experiments and simulation studies are compared and inferences are drawn.

7.1 Experimental results

Trials are conducted on the MIAB test setup and the results obtained are tabulated in Table 2.

To achieve a good weldment using MIAB welding process, the welding current and arc voltage which depend on the arc gap length are few of the most important parameters. Trials are conducted by varying the electrical

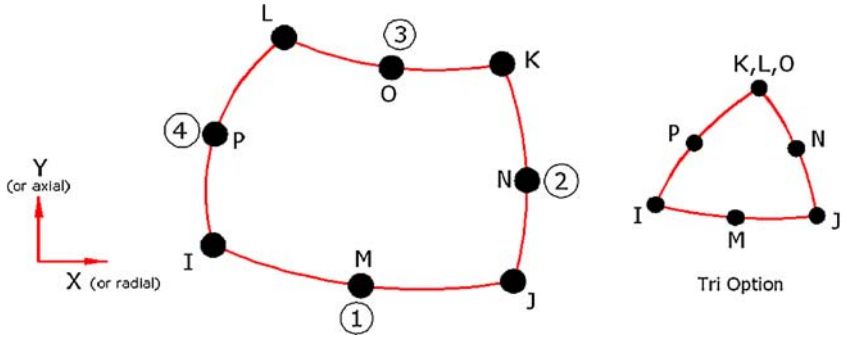

Fig. 10 Element geometry

parameters, viz., the welding voltage, welding current, magnetic coil voltage, and the magnetic coil current. Effectiveness of arc establishment and rotation is investigated by varying one of the above mentioned parameters while maintaining at least one other parameter constant. From these experiments, the following observations are made.

The arc establishment is mainly governed by the voltage of welding source. For welding voltages in the range of 15–30 V, the arc does not strike. This may possibly be due to inadequate welding current that flows to cause an arc. A voltage of above 40 V is needed to establish the adequate current to strike an arc and also to sustain the arc between the two tubes. Further trials are conducted varying the welding voltage between 45 and 50 V. In this case, arc initiation and sustenance are clearly observed. The impact of magnetizing coil voltage on the MIAB module performance is not very prominent when the coil voltage is varied between 75 and 200 V. Hence, an optimum magnetic coil voltage of around 100–110 V is considered for the trials.

The most significant factor governing the arc initiation, establishment, and the rotation is the welding current that flows through the tubes. This welding current contributes the necessary energy to the arc. This energy from the arc is distributed uniformly throughout the peripheral edges of the tubes when the arc rotates. Hence, it is necessary for the arc to possess sufficient energy to melt the tube ends. The specimen (tubes T11) possesses a high melting point. Based on rough calculations, it is estimated that the arc current should be in the range of 400–500 A to melt the material. This range of 400–500 A has been obtained taking into account the arc energy that is lost due to convection and radiation. Next, it is observed that the higher the welding current, the higher is the speed of arc rotation while maintaining the necessary welding voltage and magnetic coil voltage.

Rotation of arc at a stable speed is influenced by the magnitude and the uniform distribution of the magnetic field. Taking into account the characteristics of the magnetic field, the value of coil current is imperative for the rotation of the arc. The arc rapidly rotates along the peripheral edges of the tubes to be welded due to the electromagnetic force resulting from the interaction of

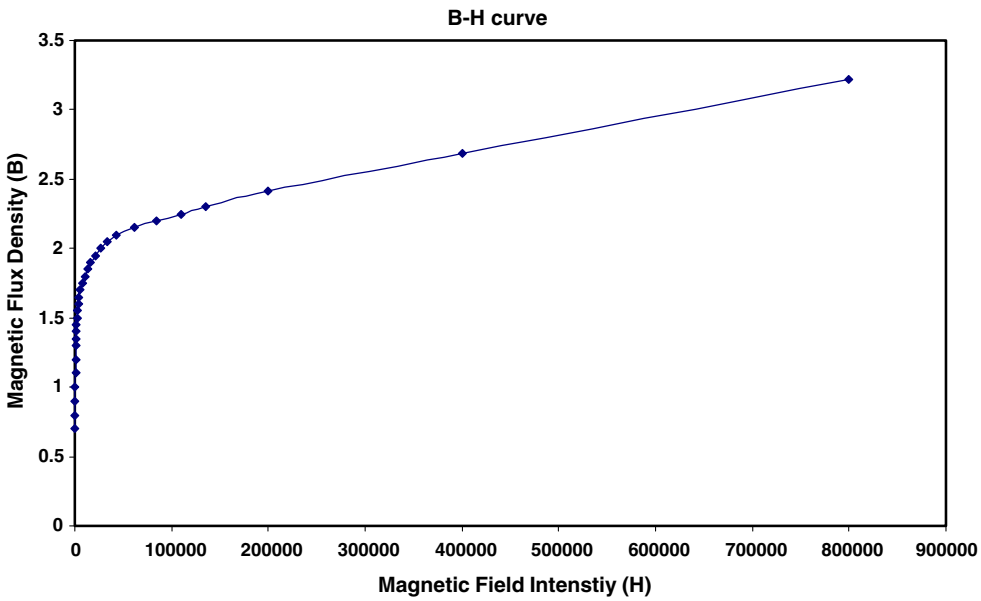

Fig. 11 B-H curve for the steel used for experimentation

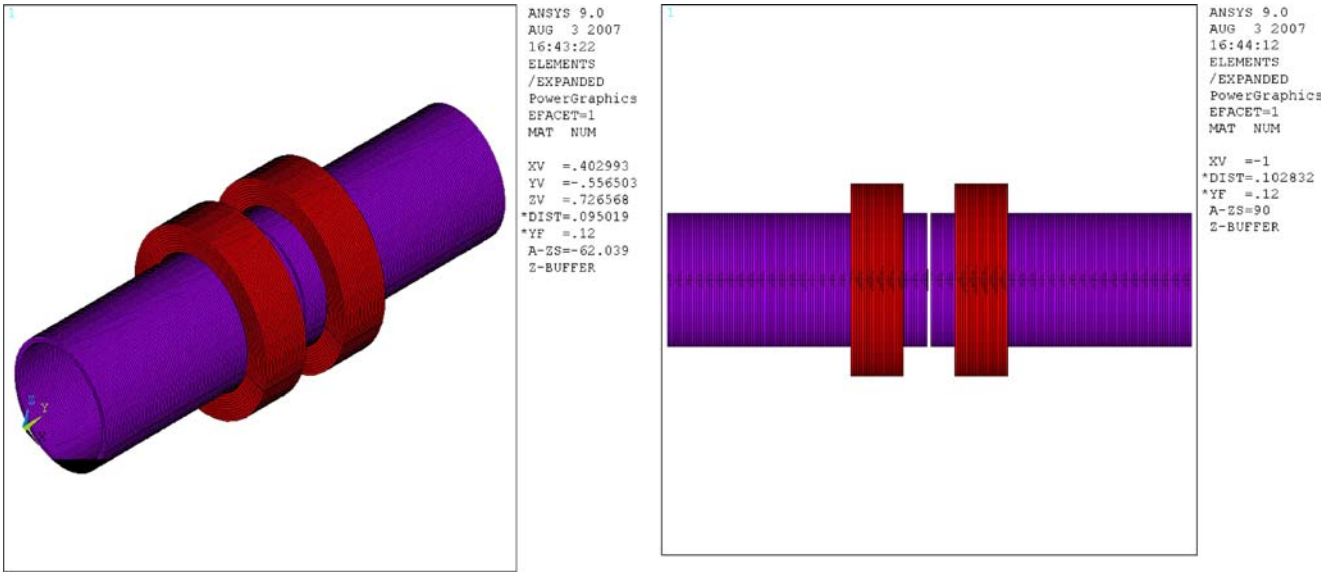

Fig. 12 Three-dimensional finite element model

Table 2 Trials on MIAB welding

Sl. no	Power source	Welding voltage (V)	Welding current (A)	Magnetic coil voltage (V)	Magnetic coil current (A)	Remarks
1	ESAB make, LAE800, Constant current	45	400	110	0.1	Arc strikes and vanishes instantaneously
2		47	400	75	0.2	Arc strikes and vanishes instantaneously
3		48	450–500	100	0.2	Arc strikes and vanishes instantaneously
4		50	400	100	0.2	Arc strikes and vanishes instantaneously
5		50	400	100	0.3	Arc strikes and vanishes instantaneously
6		50	400	100	0.3	Arc strikes and slowly vanishes
7		15	400	200–220	0.3	Arc did not strike, power supply not suitable
8		25	450	100	0.3	Arc did not strike, power supply not suitable
9		30	450	100	0.3	Arc did not strike, power supply not suitable
10		50	425	110	0.4	Half rotation of arc
11		50	450	100	0.4	Slow rotation of arc-about 60 rpm
12		50	475	100	0.4	Slow rotation of arc, about 75 rpm
13		50	500	100	0.4	Slow rotation of arc, about 90 rpm
14		50	500	100	0.5	Fast rotation of arc, about 150 rpm

the arc current and the magnetic field in the gap. This electromagnetic force is regulated by the magnetic flux density distribution in the gap between the two tubes, the arc current, and the arc length. To be precise, the magnetic flux density is the most significant parameter that governs the arc rotation and, hence, the weld quality. As already stated, magnetic flux density is established by the excitation current. Though not significant, a considerable arc rotation with about 60 rpm is observed when the exciting current is 0.3 A, while the welding voltage, welding current, and the magnetic coil voltage are 50 V, 400 A, and 100 V, respectively.

Half rotation of the arc is observed with 0.4 A exciting current, with the welding voltage, welding current, and the magnetic coil voltage held at 50 V, 425 A, and 100 V, respectively.

A slow but uniform rotation is noticed when the magnetic coil current is 0.4 A, while the welding voltage, welding current, and the magnetic coil voltage are 50 V, 450 A, and 100 V, respectively. The rotation speed increased slightly with the increase in welding current from 450 to 500 A in steps of 25 A while keeping the exciting coil current at 0.4 A. However, the speed is observed to be about 75 rpm even at this setting. Further, with the welding current at 500 A, increasing the exciting current to 0.5 A lead to a fast, uniform, and stable rotation of the arc. The reason is that the higher the coil current, the higher the magnetic flux density will be. Higher magnetic flux density leads to greater electromagnetic force, causing stronger impelling and hence fast rotation of the arc along the peripheral edges of the tubes. The major stages of the MIAB welding process are (a) before arc initiation, (b) electric arc initiation and rotation with less velocity, (c) transitory stage, when the velocity of the arc is accelerating fast, and (d) stable arc rotation stage. Figure 13 depicts these stages.

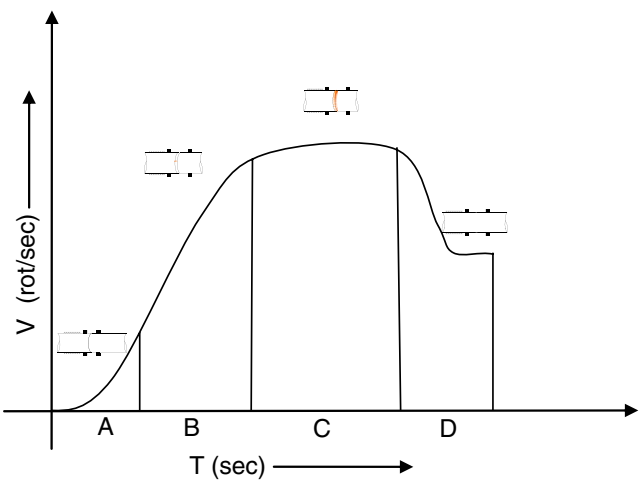

Fig. 13 Graphical representation of stages of MIAB process

7.2 Simulation result

Simulations are carried out to determine the magnetic flux distribution necessary for the magnetically impelled arc butt welding process. Initially, experimental trials are conducted to realize the principle of MIAB welding process. Trials are conducted by varying the current and voltage parameters of the welding circuit and the magnetizing circuit. It is observed that in few cases where the welding voltage is low, the arc strikes and exists for some time without vanishing instantaneously. Further, half rotation, slow, and fast rotation is noticed when the exciting current is increased. From this result, a conclusion is drawn that the magnetic flux density increases with the increase in the exciting current. This clearly emphasizes the linearity property existing between exciting current and the magnetic flux density. As the magnetic flux density increases, electromagnetic force increases, leading to a fast and uniform rotation of the arc along the peripheral edges of the tubes. The simulations mainly focus on the prediction of the value of magnetic flux density which is necessary in order to obtain slow rotation and fast rotation. Simulation is carried out by using a finite element code ANSYS.

7.2.1 Simulation of magnetic flux density distribution in case of slow rotation of arc

The input conditions for the simulation for this particular case are the same as that of the 11th trial conducted in our experiment. The values of welding current, welding voltage, magnetic oil voltage, and magnetic coil current are 450 A, 50 V, 100 V, and 0.4 A, respectively. Though slow rotation is observed in the 11th, 12th, and 13th trials, the 11th trial is considered for simulation, as we observe the slow rotation initially under this case and the input is minimum compared to that of the 12th and 13th trials.

The magnetic flux distribution in a two-dimensional finite element is shown in Fig. 14. It is seen that the magnetic flux density is highly concentrated at the center between the two tubes. It gradually decreases away from the center. The gap between the two tubes is maintained at 2 mm in the experimental setup. This two-dimensional finite element model is a simpler version to examine the results.

Figure 15 shows the three-dimensional FEM model of the setup to determine the magnetic flux distribution for MIAB welding process. The maximum flux density is found to be 2.032 T from the simulations. Simulations reveal that the minimum magnetic flux density required to accomplish slow rotation of arc is 2.032 T. This maximum flux density is concentrated at the center between the two aligned tubes for MIAB welding. It can be noted that the magnitude of flux density decreases from the center.

Figure 16 shows the variation of the magnetic flux density with radial distance. The magnetic flux density is

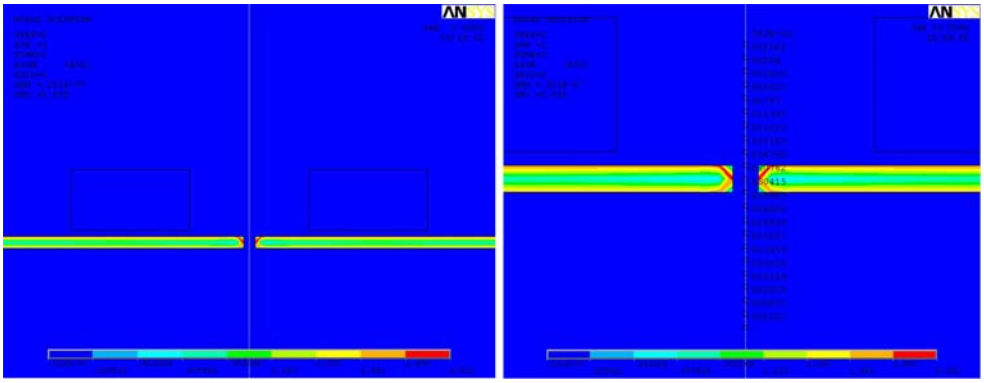

Fig. 14 Two-dimensional finite element model

minimum at the bottom of the peripheral edge of the tubes and is observed to be 0.799 T when the welding current, welding voltage, magnetic oil voltage, and magnetic coil current are 450 A, 50 V, 100 V, and 0.4 A, respectively. Then, gradually, the flux density increases and attains the peak value of 7.976 T at the center. Further, the value of flux density decreases to almost zero at the top of the exterior edge of the tubes.

Figure 17a illustrates the distribution of magnetic flux lines when the arc is slowly rotating at a speed of about 60 rpm and the exciting current is 0.4 A. It can be noticed that the flux lines are concentrated more at the gap between the two pipes leading to the reinforced electromagnetic force, which facilitates arc rotation at a requisite high speed. The flux lines are restricted within the boundary of the MIAB welding system. Figure 17b shows the results of the experiments in which the magnetic flux lines are generated at the tube joint [14].

7.2.2 Simulation of electromagnetic force distribution in case of slow rotation of arc

It is emphasized in the previous sections of this paper that in MIAB welding, an electric arc is scanned across the faying surfaces in the gap between the tubes to be welded. The arc is impelled along the peripheral edges of the tubes by an electromagnetic force. From Eq. 1, it is clear that the electromagnetic force is mainly governed by the magnetic flux density in the tube gap, the welding current, and arc length. The force exerted on the flowing current influences the acceleration of the rotating arc. Hence, it is obvious that by adjusting the strength of the magnetic field, the magnitude of the arc current, or the width of the arc gap, the electromagnetic force is altered, which in turn administers the speed of the arc. The ability to alter the speed of the arc by changing the electromagnetic force plays a significant role in MIAB welding process. In particular, by sharply increasing the current (to about three times) for a very short time just prior to upset, a rapid expulsion of molten metal occurs, which provides cleaning action. This eliminates the need for shielding gas. The direction of the force is determined by applying Fleming's left hand rule, which states that the rotating direction of the arc is always perpendicular to the applied magnetic field and the arc current, as shown previously in Fig. 2.

It is clearly noticed from the principle that the arc rotation indirectly depends on the magnetic flux distribution which varies with the varying exciting current in the coils [5]. The higher the exciting current, the larger the magnetic field would be, thereby obtaining the stronger electromagnetic force. Hence, the arc speed increases which uniformly heats and melts the pipe ends. This leads to better welding and enhanced weld quality as shown in the macrograph (Fig. 18b). However, when the magnetic flux density was comparatively low, the electromagnetic force created was less, leading to slow arc rotation and poor quality weld as shown in Fig. 18a. This emphasizes that magnetic flux density governs the MIAB welding process, and hence, this parameter was chosen for simulation by varying other system parameters of MIAB.

Since electromagnetic force is one of the major parameters assisting the MIAB process, an attempt is made

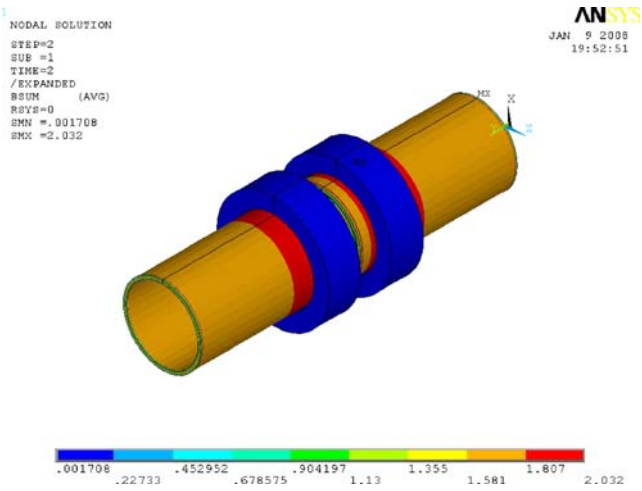

Fig. 15 Three-dimensional finite element model

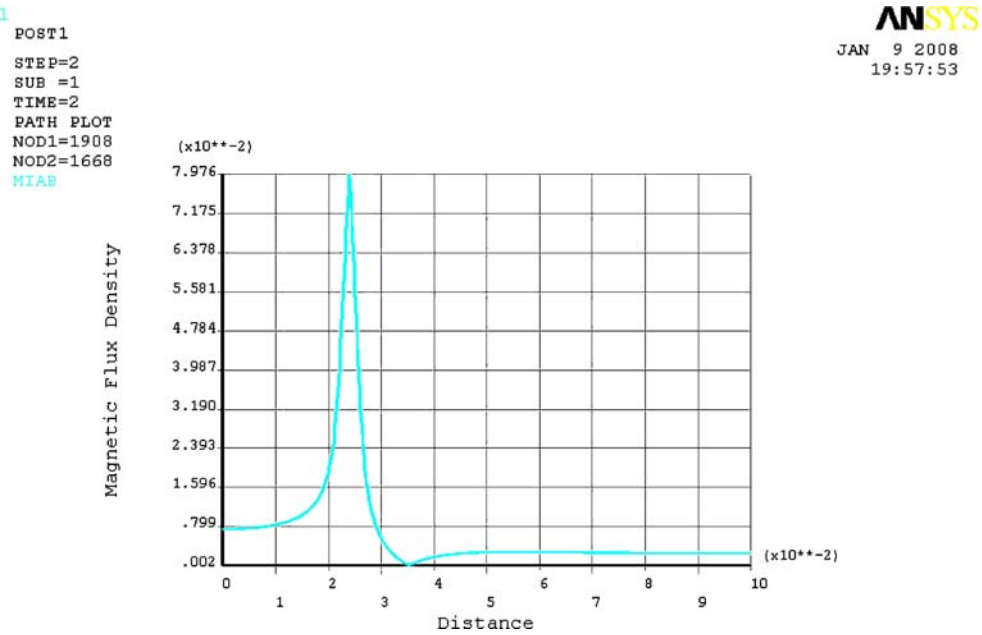

Fig. 16 Variation of magnetic flux density versus the radial distance from the center

in this work to develop a three-dimensional FE analysis and to explore the electromagnetic force distribution when the arc rotation speed is slow (input to three-dimensional model as per 11th experimental trail). The simulation result clearly emphasizes that the force is acting outwards and perpendicular to the direction of welding current and the magnetic flux density. Figure 19 shows the force acting on the peripheral edge of a single tube. Maximum force is concentrated in the arc gap region where the magnetic flux density is maximum. From the result, it is evident that force is directly proportional to the magnetic field. In addition, it can be noted that the force distribution is uniform along the peripheral edges of the tubes to be welded. This leads to uniform arc rotation speed, producing an enhanced quality weld. The maximum magnitude of electromagnetic force near the tube edges is 1.059 electromagnetic units for slow rotation of the arc.

Similarly, Fig. 20 shows the force acting in the arc region along the two tube edges. It can be clearly noticed that the electromagnetic force distribution is forced outwards. This impels the arc along the edges and also pushes the arc from the inner diameter to the outer diameter for uniform heating, leading to the achievement of good weld.

The force occurs due to the magnetic flux lines generated by the flowing current interacting with the magnetic flux lines of the applied magnetic field. This phenomenon is shown graphically in Fig. 21, which depicts a current carrying conductor under the influence of an applied magnetic field. The force is generated on the side of the conductor where the magnetic flux lines are aligned. Ironically, in arc welding processes, a similar interaction creates a phenomenon called "arc blow," often a detriment to the process. Initially, when MIAB is welding a

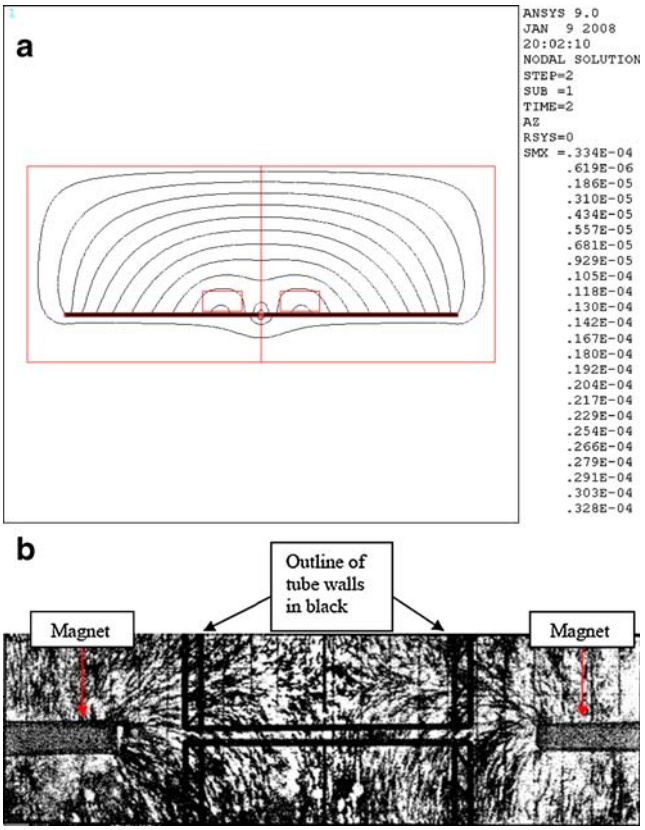

Fig. 17 Distribution of magnetic flux lines in the pipe gap region

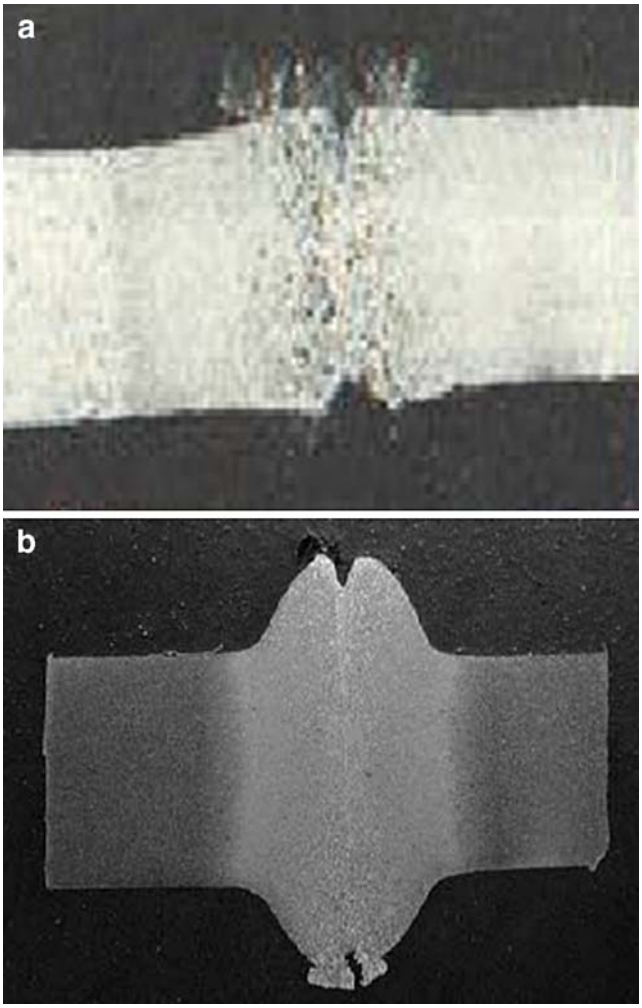

Fig. 18 Macrograph of weld joint of MIAB process [5]

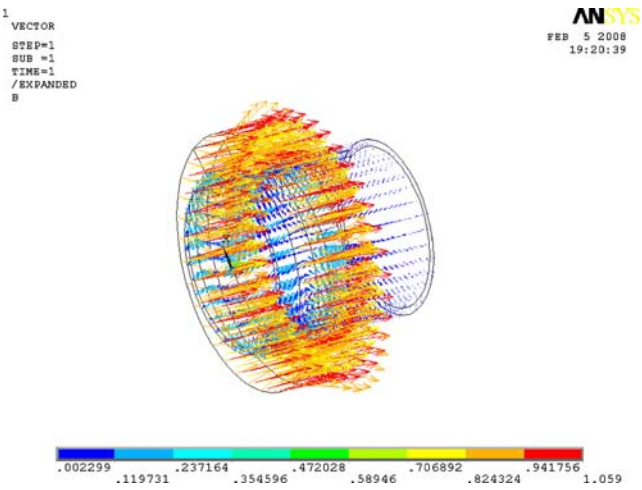

Fig. 19 Electromagnetic force acting on the peripheral edge of a single tube

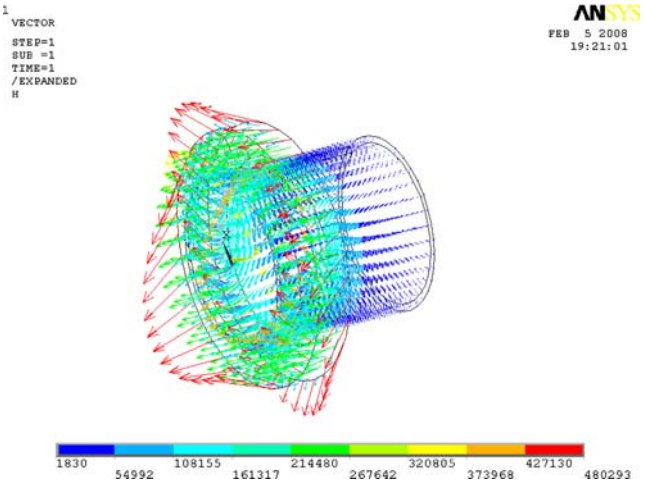

Fig. 20 Electromagnetic force distribution in the tube gap region

ferromagnetic material, the arc is pushed to the inner diameter (ID) of the joint due to arc blow. Upon heating, the curie temperature is first reached on the ID of the tube, altering the distribution of magnetic flux in the joint and pushing the arc outward as shown in Fig. 22. The outward movement of the arc can play an important role in generating uniform heating at the joint as shown in Fig. 23.

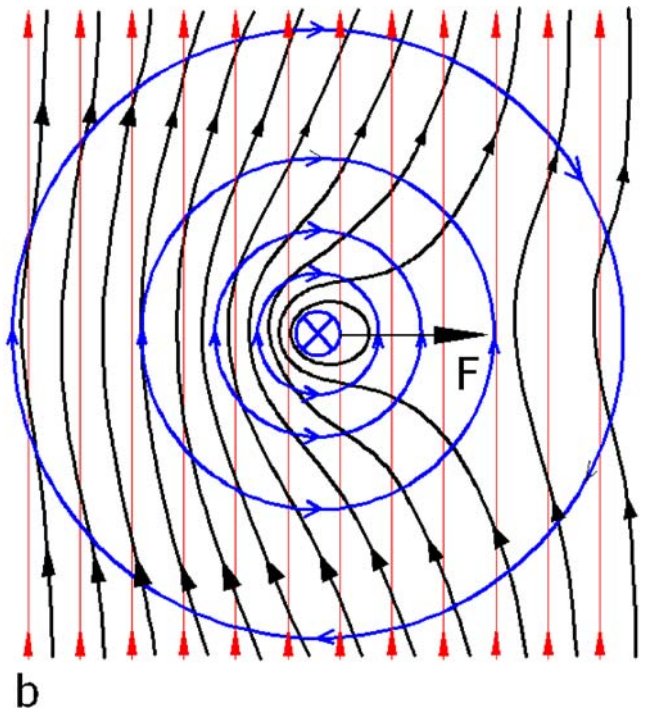

Fig. 21 Aligned magnetic flux lines create force on conductor [1]

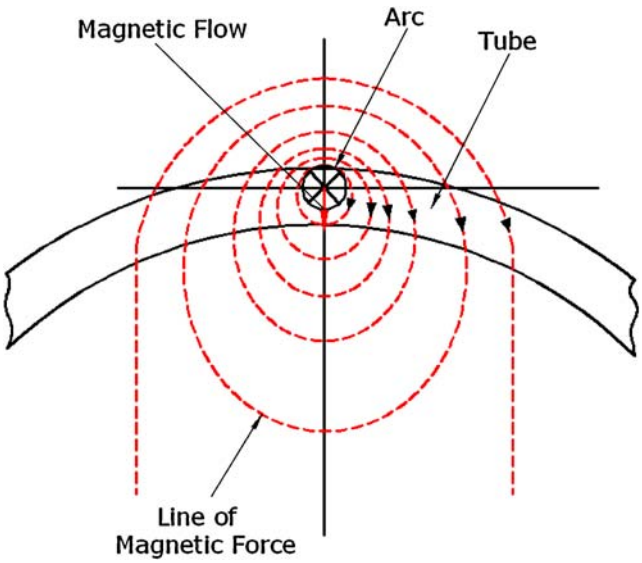

Fig. 22 Magnetic arc blow due to tube geometry effects [15]

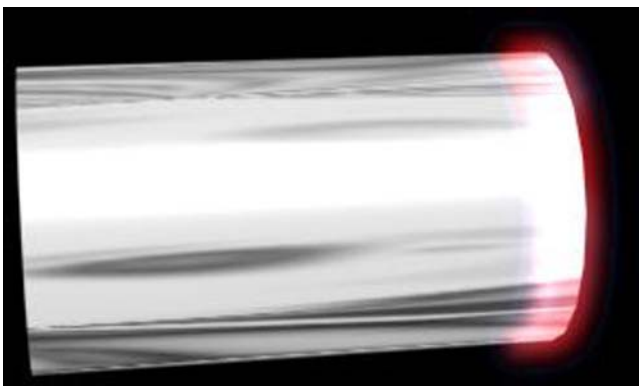

Fig. 23 Uniform heating at the tube edge (joint)

8 Validation of simulation result

The results of FEA are validated with the experimental data. In the experiments, the radial magnetic flux density was measured using a Gauss meter at the various positions from the pipe surface as shown in Fig. 24. The Gauss meter was initially taken from the outside edge to the inner edge and vice versa for the determination of magnetic flux density between the steel tubes. It was observed that the maximum magnetic flux density noted for slow arc rotation with the input considered as in case of the 11th trial in experimentation is 2.018 T. The values of maximum magnetic flux density that was determined in simulation for slow arc rotation is 2.032 T, which are almost equivalent to that of the experimental data. The facility for measuring the electromagnetic force is presently not available at this laboratory; hence, the validation of the FE electromagnetic force simulation result could not be performed. However, this FE analysis of the force distribution in MIAB welding would certainly facilitate the researchers working on numerical analysis of MIAB welding. The results of numerical analysis have an excellent correlation with that of the experimental ones.

9 Conclusions

A prototype MIAB laboratory module is designed and tested at the Welding Research Institute, Bharat Heavy Electricals Limited, Trichy-India. On investigation, it is identified that the magnetic flux density was one of the significant factors that affects the electromagnetic force which in turn influences the arc rotation behavior in MIAB welding. Thus, the effective design of the electromagnetic system is an essential task for the construction of the MIAB welding machine. Several trials are conducted on different magnetic coil systems by varying the welding current and arc voltage. The test results are discussed.

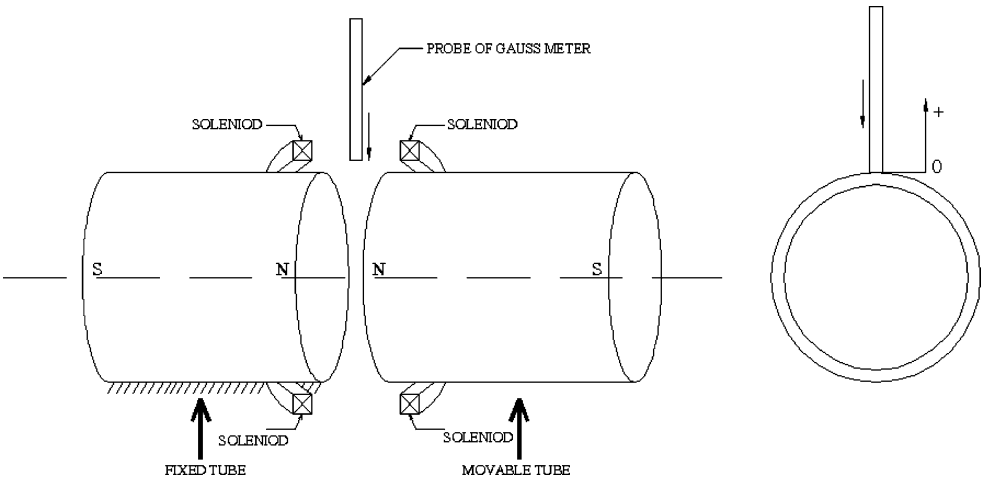

Fig. 24 Measuring method for magnetic flux density [3]

The present prototype produces a continuous and uniform arc rotation. The numerical analysis of magnetic flux density and electromagnetic force distribution, respectively, helps in thoroughly understanding the MIAB welding process and further facilitates in optimizing the design and development of the electromagnetic system. In this work, the minimum value of exciting current in the coil and the corresponding magnetic flux density and electromagnetic force distribution, respectively, for MIAB welding process are investigated. These are determined in a parallel manner by numerical analysis using the finite element code ANSYS. Further, the simulation results were validated with the experimental data with respect to magnetic flux density. The following conclusions are drawn from the results of the analysis:

- The minimum magnetic flux density that is required to accomplish slow rotation of arc is 2.032 T for 0.4 A exciting current in the magnetic coil system.
- By using the numerical model, the magnetic flux density distribution and electromagnetic force distribution for different exciting currents and welding currents could be analyzed. It is revealed that the magnetic flux density in the gap between the pipes increases with increasing exciting current.
- The results of the simulation on electromagnetic force would facilitate the comprehensive understanding of the arc movement from the inner diameter to the outer diameter.
- The electromagnetic force analysis emphasizes that the speed of arc rotation is governed by the magnitude of force. Furthermore, it can be noticed that higher the force, greater is the speed and the better is the weld quality.
- The results from the analysis are compared with those from the available experimental data, and it is found that the results of numerical analysis are in excellent agreement with experimental results.

Acknowledgments The authors thank Head, Welding Research Institute and Management, Bharat Heavy Electricals Limited, Tiruchirappalli for extending the facilities to carry out this research work and allowing to present the results in this paper. The authors thank NITT for providing computation facilities.

References

1. Ganowski F-J (1974) The magnet arc welding process. Weld Metal Fabr 42:206–213 (June)
2. Georgescu V, Iordachescu D, Geogescu B (2000) Pneumatically operated equipment for pressure welding in magnetic forces field. Dunarea De Jos, University of Galati, Romania
3. Glickstein SS (1979) Arc modelling for welding analysis. Westinghouse–Bettis Atomic Power Laboratory. West Mifflin, USA, Paper 5, pp 1–16
4. Kim JW, Choi DH (2003) A study on the numerical analysis of magnetic flux density distribution by a solenoid for magnetically impelled arc but welding. . Proc Inst Mech Eng Part B: J Eng Manuf 217:1401–1407
5. Arungalai Vendan S, Manoharan S, Buvanashekaran G, Nagamani C (2008) Simulation of magnetic flux distribution for magnetically impelled arc butt welding of steel pipes. Int J Multidisc Model Mater Struct 222:1783–1790
6. Arungalai Vendan S, Manoharan S, Buvanashekaran G, Nagamani C (2008) Magnetic flux distribution modeling of magnetically impelled arc butt welding of steel tubes using finite element analysis. Inst Mech Eng, Part C: J Mech Eng Sci (in press)
7. Georgescu V, Iordachescu D (1998–2000) Original magnetizing systems for ROTARC welding. The Annals of Dunarea de Jos, University of Galati, pp 10–14 (ISSN 1221-4639)
8. Schlebeck E (1978) Welding with a magnetically moved arc (MBL welding): a new means of rationalization. Proceedings of Welding Institute Conference on Advances in Welding Processes. Harrogate, pp 249–256
9. Kuchuk-Yatsenko SI, Kachinsky VS, Ignatenko VYu (2002) Magnetically-impelled arc butt welding of thick-walled pipes. Paton Weld J 7:24–28
10. Kachinskiy VS, Krivenko VG, Ignatenko VYu (2002) Magnetically impelled arc butt welding of hollow and solid parts. Commission III Doc IIW-1564-02, pp 49–56
11. Johnson KI, Carter AW, Dinsdale WO, Threadgill PL, Wright JA (1979) The magnetically impelled arc butt welding of mild steel tubing. Weld J 59(11):17–27
12. Tagaki K, Arakida F, Miyamori H, Ozawa M (1986) Arc rotating phenomena in rotating arc butt welding of steel pipes. J Jap Weld Soc 4(2):305–311 (in Japanese)
13. Mori S, Yasuda K (1990) Magnetically-impelled arc butt welding of aluminum pipes. Trans Jpn Weld Soc 21(1):3–10
14. Schmidt N (1986) Magnetic field distribution during pressure welding of magnetic and non-magnetic components with a magnetically controlled arc, welding and cutting. 10/1986, pp E169–E171
15. Sato K, Ioka O (1991) An experimental study of rotational behavior of the arc during magnetically impelled arc butt welding. Weld Int 5(1):5–10